J Mater Sci (2013) 48:651–658
DOI 10.1007/s10853-012-6770-y

CdSe/$Cd_{1-x}Zn_xS$ core/shell quantum dots with tunable emission: growth and morphology evolution

Ping Yang · Shiquan Wang · Masanori Ando · Norio Murase

Received: 4 May 2012 / Accepted: 25 July 2012 / Published online: 8 August 2012

Abstract We demonstrate an organic synthesis to fabricate hydrophobic core/shell CdSe/$Cd_{1-x}Zn_xS$ quantum dots (QDs) with tunable photoluminescence (PL) between green and red at relatively low temperature using trioctylphosphine S reacted directly with cadmium and zinc acetate. A seeded growth strategy was used for preparing large CdSe cores. Large CdSe cores revealed a rod-like morphology while small one exhibited a spherical shape. Being coated with a $Cd_{1-x}Zn_xS$ shell on spherical CdSe cores with an average size of 3.9 nm in diameter, core/shell QDs exhibited a cubic morphology (a length of 5 nm). In contrast, the core/shell QDs created using a small core (3.3 nm in diameter) show a spherical morphology. Namely, the anisotropic aggregation behavior of CdS monomers on CdSe cores occurs when the rod-like core is coated with a $Cd_{1-x}Zn_xS$ shell. CdS interlayer plays an important role for such morphology evolution because all CdSe cores with a pure ZnS shell exhibited a spherical morphology. The PL properties of CdSe/$Cd_{1-x}Zn_xS$ core/shell QDs depended strongly on the size and morphology of the cores. The QDs revealed a narrow and tunable PL spectrum. It is believed that this facile strategy can be extended to synthesize other core–shell QDs at low temperature.

P. Yang · S. Wang · M. Ando · N. Murase (✉)
Health Research Institute, National Institute of Advanced Industrial Science and Technology (AIST), Midorigaoka, Ikeda-city, Osaka 563-8577, Japan
e-mail: n-murase@aist.go.jp

P. Yang
School of Material Science and Engineering, University of Jinan, 250022 Jinan, People's Republic of China

Present Address:
N. Murase
Health Research Institute, National Institute of Advanced Industrial Science and Technology (AIST), 2217-14, Hayashi-cho, Takamatsu, Kagawa 761-0395, Japan

Introduction

Semiconductor quantum dots (QDs) with tunable photoluminescence (PL) in a region of UV–Vis–near infrared emission are of great interest and have been widely investigated due to their potential applications such as optoelectronic devices, lasers, and biomedical tags [1]. The optical and electrical properties of QDs strongly depend on their morphologies and structures in a nanometer scale. For example, the band gap energy of nanostructures, and consequently their emission wavelength, is typically strongly dependent on the diameter of the rod and only weakly dependent on its length [2]. The properties of nanostructures are governed by the decrease in the confinement of charge carriers along the length axis and by the cylindrical symmetry of the particles. Fabrication of high-quality QDs with desired morphology is of great fundamental and technological interest [3]. In particular, the direct fabrication of complex nanostructures with various morphologies in nanoscale is one of the most challenging topics due to the possibility to design new materials and devices with desired properties.

Nanocrystals with special morphologies such as rod-like and triangle show interesting chemistry and are located among zero-dimensional QDs to two- and three-dimensional nanostructures. The most apparent nature of the QDs with special morphologies is their lower PL efficiencies [2]. Since wet chemical synthesis techniques have resulted in homogeneous size distributions, high quantum yields, and safer precursor materials, great progress has been made in the fabrication of luminescent semiconductor nanocrystals with

one-dimensional (1D) nanostructure [4]. Anisotropic growth of unique crystal facets results in 1D nanostructures with various diameters and lengths. To passivate most of the surface defects and increase both the PL efficiency and the stability, a shell of a higher band gap semiconductor needs to be epitaxially grown on the core surface. A facile method for obtaining nano architecture of core/shell systems is through a seeded growth approach. Such approach also made the growth of a shell of a higher band gap inorganic material on a core of another lower band gap material to form a heterostructure for the purpose of surface modification. For example, CdSe spherical cores encapsulated in CdS rods, forming type-I and quasi-type-II systems, and ZnSe cores embedded in CdS rods forming a type-II system have been reported [5, 6].

Within the rapidly advancing research in colloidal nanocrystals of II–VI, III–V, and IV–VI semiconductors for applications in biology and materials science, CdSe is still one of the most popular QDs created by various chemical strategies. Bulk CdSe has two crystalline lattice structures: wurtzite (hexagonal) and zinc blende (cubic). Bandgap of QDs composed of CdSe ($E_g = 1.76$ eV, $a_B = 9.6$ nm) can be tuned through quantum confinement to emit visible fluorescent spectrum. Depending on the specific application requirements, different semiconductor materials have been exploited for the shell-growth on CdSe cores, for instance single shell CdS, ZnS, ZnSe, and ZnTe and a double shell CdS/ZnS and ZnSe/ZnS [7–11], where the outer ZnS shell serves as a potential barrier to confine the charge carriers inside the core regions. The main method for preparing such QDs is by classical colloidal chemistry, where various researchers have employed organometallic and/or metal organic compounds under anaerobic conditions. For example, CdSe QDs was prepared by reacting dimethylcadmium ($CdMe_2$) with trioctylphosphine selenium (TOPSe) in TOP/trioctylphosphine oxide (TOPO) at high temperature [12]. Other researchers used single-molecular precursors such as bis(diethyldithio-/diselenocarbamato) Cd(II)/Zn(II) for the preparation of CdSe/ZnS QDs. Therefore, the application of a novel strategy, which uses relatively nontoxic chemicals, to the preparation of CdSe based QDs at low temperature is highly desirable.

Growth mechanisms of CdSe quantum rods and CdTe tetrapods have been explained by the preferential attachment of ligands to certain crystal facets, precursor concentrations and temperature dependent crystal phase growth [13, 14]. The crystal growth mechanisms of nanomaterials consists of four parts including initial nucleation based on critical concentration precipitation, monomer diffusion, and addition to nucleated sites, ligand preferential binding characteristics, and inherent crystal facet potential energy [4]. A seeded growth mechanism makes us to create large QDs with a narrow size distribution. The ability to engineer the band gap energy of QDs has led to the development of nanomaterials with many new exciting properties and 1D nanostructure. For example, CdSe/CdS/ZnS nanorods with CdSe rod core and CdS/ZnS graded shell have been fabricated [15, 16]. To fully exploit the potential advantages of QDs in properties, semiconductor nanostructures with controlled morphologies are still expected. High degrees of synthetic control are necessary for both fundamental and device investigations, but the mechanisms of nanocrystal growth are not completely understood.

Very recently, we prepared core/shell CdSe/$Cd_{1-x}Zn_xS$ QDs with bright and tunable PL by an organic synthesis at high temperature using cadmium oxide, cadmium acetate dihydrate, zinc acetate, octadecylphosphonic acid, trioctylamine, oleic acid, TOPSe, and TOPS [17]. In this paper, we demonstrated the preparation of core/shell CdSe/$Cd_{1-x}Zn_xS$ QDs using hexadecylamine (HDA) as a capping agent at relatively low temperature. The morphologies and PL properties of the QDs depended strongly on the sizes and morphologies of CdSe cores. In addition, a seeded growth approach at relatively low temperature have been developed to fabricate rod-like CdSe cores, which we have successfully applied to the synthesis of core/shell CdSe/$Cd_{1-x}Zn_xS$ QDs with red PL (peak wavelength of 643 nm). To indicate the evolution mechanism of morphology, CdSe cores were coated with a ZnS shell. Comparison with CdSe/$Cd_{1-x}Zn_xS$ QDs, CdSe/ZnS QDs revealed a smaller red-shifted of PL spectra. All CdSe/ZnS QDs exhibited a spherical morphology.

Materials and methods

Chemicals and materials

Stearic acid, cadmium oxide (CdO), 1-octadecene (ODE), trioctylphosphine (TOP, 97 %), selenium (99.5 %, 100 mesh), sulfur (99.98 %, powder), cadmium acetate dihydrate ($Cd(Ac)_2 2H_2O$ 98 %), zinc acetate ($Zn(Ac)_2$, 99.99 %), and HDA were supplied from Sigma Aldrich. All the chemicals were of analytical grade or of the highest purity available, and used directly without any further purification. The pure water was obtained from a Milli-Q synthesis system (resistivity of 18.2 MΩ cm).

Preparation of CdSe cores

CdSe cores were prepared by a hot injection approach. Typically, 30 mg of CdO, 1 g of stearic acid, and 7 mL of ODE were loaded into a three-neck flask (50 mL) under N_2 flow, and stirred at 255 °C until CdO was completely dissolved. Se powder (80 mg) was dissolved in 1 mL of TOP. The TOPSe solution was then injected into the

Table 1 Preparation conditions and properties of CdSe cores

Sample	Reaction time (min)	Injection speed (mL/min)[a]	Morphology	Average diameter (nm)	PL peak wavelength (nm)	PL efficiency (%)	FWHM (nm)
1	2.5	2	Spherical	3.0	586.4	2.31	33.4
2[b]	3	1	Spherical	3.7	600	N/A	N/A
3[c]	6	0.3	Rod-like	4.0	607	0.24	40.8

[a] The injection speed of TOPSe

[b] It is difficult to estimated the PL properties because the PL of Sample 2 is too weak

[c] Sample 3 (CdSe cores) was prepared by Sample 1 as seeds

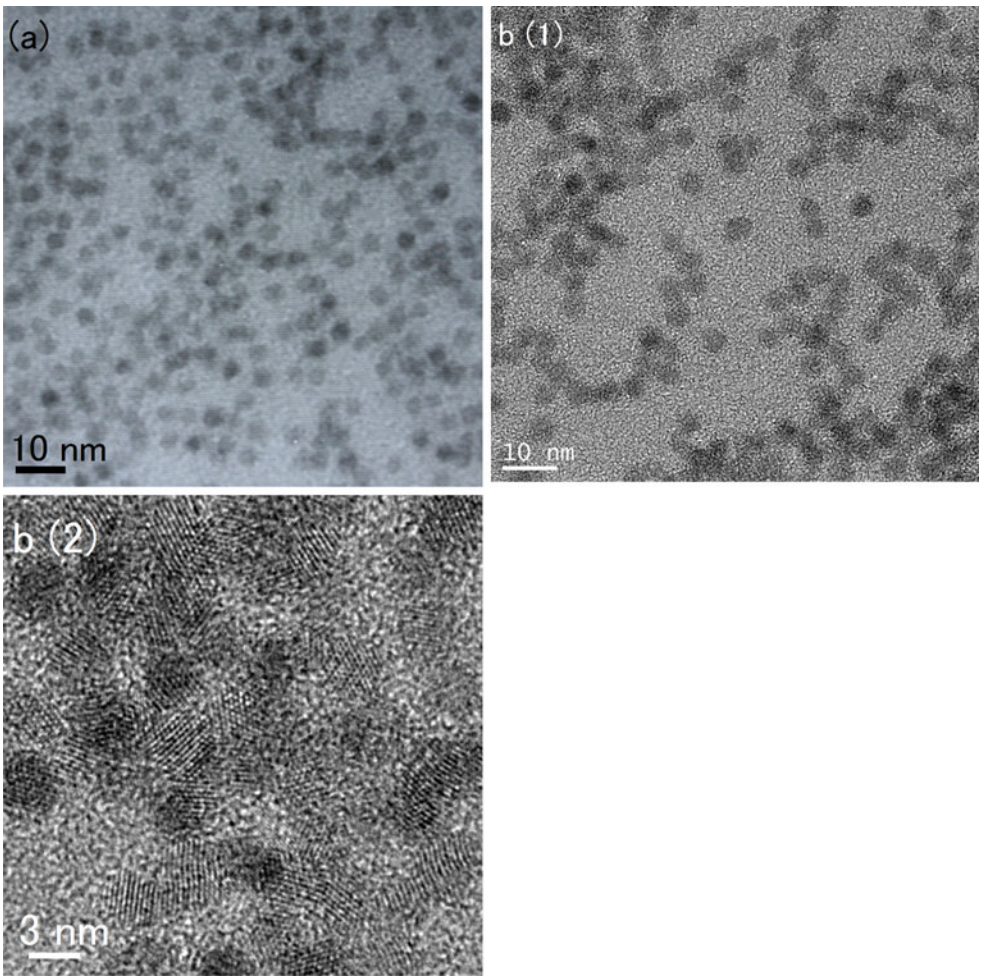

Fig. 1 TEM images of CdSe cores shown in Table 1. **a** Sample 1. **b** Sample 2. Well-developed lattice fringes of CdSe cores were observed in **b** (2)

cadmium precursor solution with rapid stirring, and kept at 255 °C for several minutes, followed by cooling down to room temperature. 10 mL of hexane and 60 mL of ethanol were added to precipitate the CdSe QDs. The product was then washed with copious ethanol, re-dispersed in 20 mL of toluene, and centrifuged at 15,000 rpm for 15 min to remove the sludge. Next, the CdSe cores were precipitated with ethanol, and re-dispersed in 10 mL of toluene for subsequent preparation of large cores and shell coating. To prepare CdSe cores with different sizes, the reaction time and injection speed of TOPSe were adjusted. The preparation conditions are summarized in Table 1.

To prepare CdSe cores with large size, a seed growth approach was used. Briefly, 16 mg of CdO, 1 g of stearic

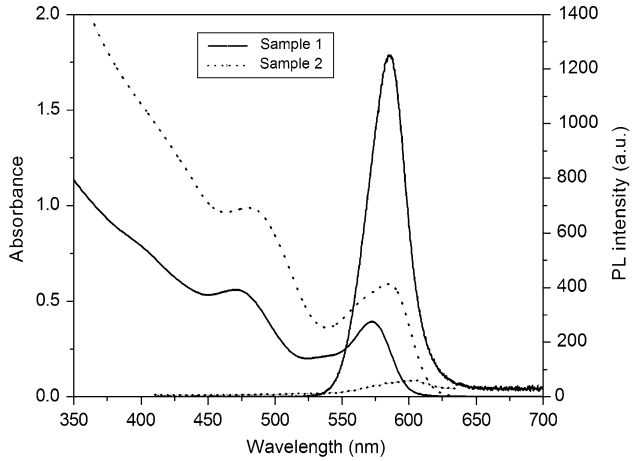

Fig. 2 Absorption and PL spectra of CdSe cores (Samples 1 and 2 shown in Table 1). Compared with Sample 1, Sample 2 revealed red-shifted absorption and PL peak. However, the PL of Sample 2 was weak

acid, and 7 mL of ODE were loaded into a three-neck flask (50 mL) under N_2 flow, and stirred at 255 °C until the CdO completely dissolved. The toluene solution of small CdSe cores (3 mL) was injected directly into the cadmium precursor solution with vigorous stirring. When the temperature of the solution was back to 255 °C, a TOPSe solution (1 mL) with 70 mg of Se was injected within 3 min. The reaction was terminated by cooling after further 3 min. The resulting sample was purified and re-dispersed by the same procedure with small cores.

Preparation of core/shell CdSe/$Cd_xZn_{1-x}S$ and CdSe/ZnS QDs

The preparation of $Cd_xZn_{1-x}S$ shell was performed by directly reacting cadmium and zinc acetate with TOPS. In a typical synthesis, 14 mg of $Cd(Ac)_2 2H_2O$, 10 mg of

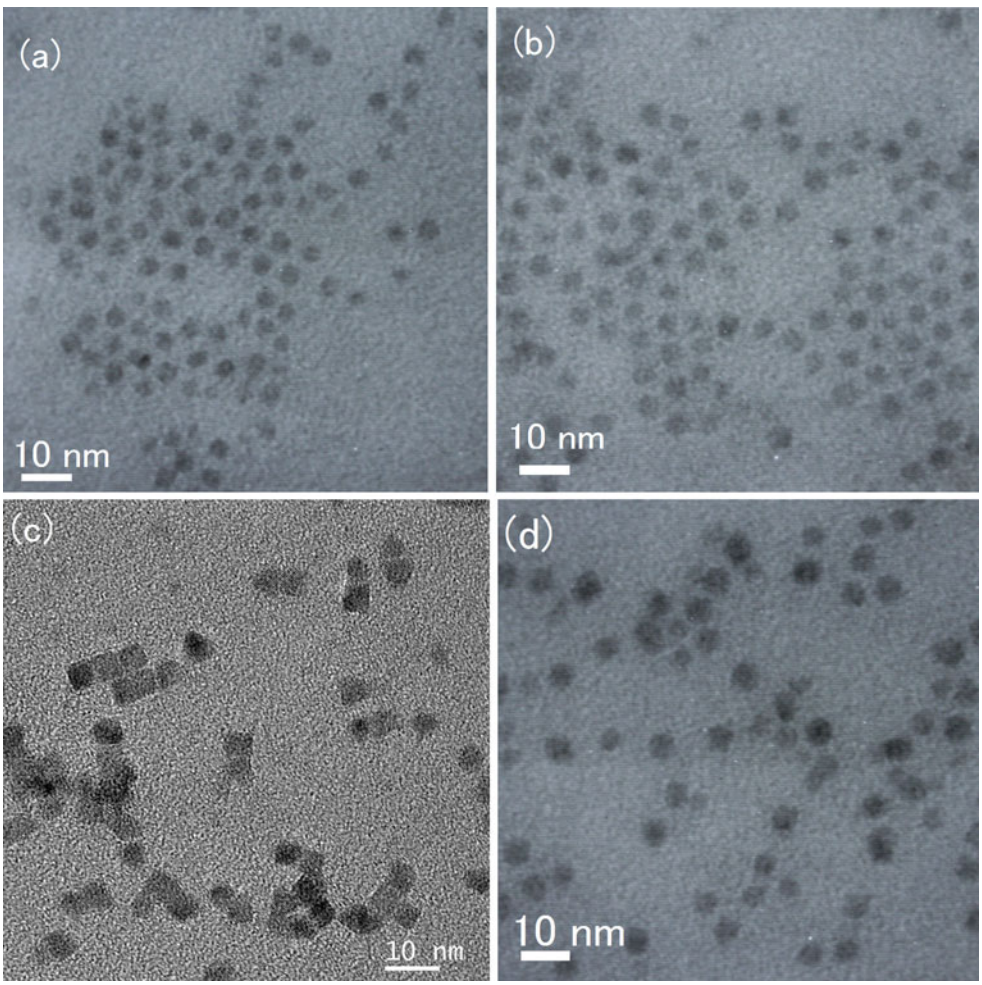

Fig. 3 TEM images of CdSe cores with a CdZnS and ZnS shell shown in Table 2. **a** Sample 4 (CdSe/$Cd_{1-x}Zn_xS$). **b** Sample 5 (CdSe/ZnS). **c** Sample 6 (CdSe/$Cd_{1-x}Zn_xS$). **d** Sample 7 (CdSe/ZnS)

Table 2 Preparation conditions and properties of core–shell QDs

Sample	Core[a]	Shell	Morphology	PL efficiency (%)	PL peak wavelength (nm)	FWHM (nm)
4	1	$Cd_{1-x}Zn_xS$	Spherical	19	602	40.0
5	1	ZnS	Spherical	36	596	37.8
6	2	$Cd_{1-x}Zn_xS$	Cubic	26	627	39.6
7	2	ZnS	Spherical	33	619	41.8
8	3	$Cd_{1-x}Zn_xS$	Spherical	18	643	34.4
9	3	ZnS	Spherical	19	627	30.8

The reflux time of these core/shell QDs is 10 min

[a] CdSe cores shown in Table 1

$Zn(Ac)_2$, 0.5 mg of HDA, and 7 mL of ODE were placed in a three-neck round-bottom flask under N_2 flow, and stirred at 220 °C until the Cd and Zn salts were completely dissolved. 6 mg of S powder was dissolved in 0.5 mL of TOP. The toluene solution of CdSe cores (3 mL) was injected with vigorous stirring, followed by the injection of the TOPS solution. The mixture was kept at 240 °C with stirring for 15 min, followed by cooling down to room temperature. The products were precipitated, washed twice with ethanol, and re-dispersed in 10 mL of toluene. To prepare CdSe/ZnS QDs, $Cd(Ac)_2 2H_2O$ was removed from the reaction system.

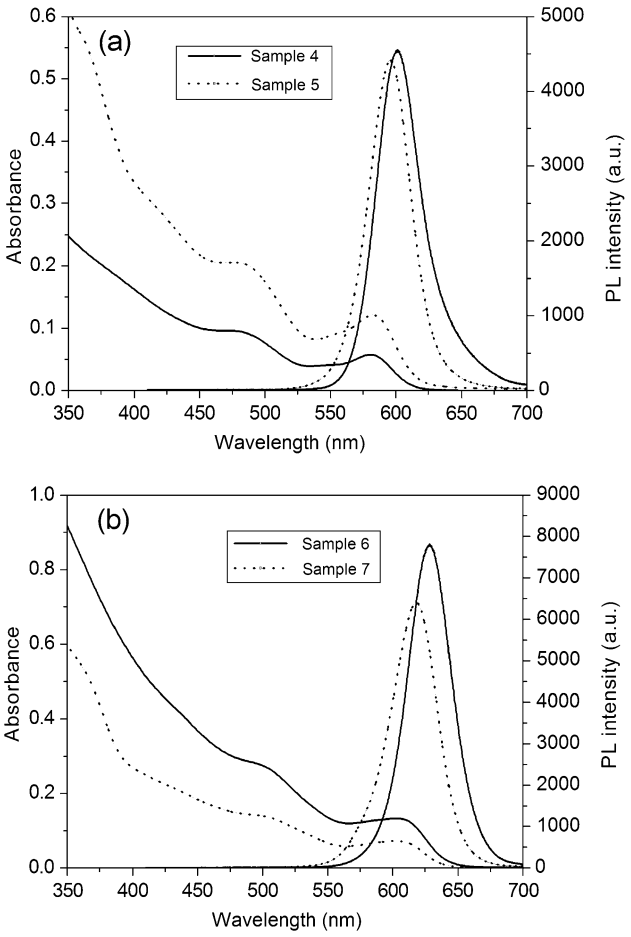

Fig. 4 Absorption and PL spectra of of CdSe cores with a CdZnS and ZnS shell shown in Table 2. **a** Samples 4 (CdSe/$Cd_{1-x}Zn_xS$) and 5 (CdSe/ZnS). **b** Samples 6 (CdSe/$Cd_{1-x}Zn_xS$) and 7 (CdSe/ZnS)

Apparatus

The absorption and PL spectra were recorded using conventional spectrometers (Hitachi U-4000 and F-4500, respectively). Both of excitation and emission slits are 5 nm for the measurement of PL spectra. The transmission electron microscopy (TEM) observations of samples were carried out with a Hitachi EF-1000 electron microscope. The PL efficiencies of samples in solution were estimated using a method previously reported [18, 19]. Briefly, the PL and absorption spectra of a standard quinine solution (quinine in 0.1-N H_2SO_4 solution; PL efficiency η_0 of 55 %) were measured in a 1-cm quartz cell as a function of the concentration. The emission intensity (in units of the number of photons) is expressed as below.

$$P_0 = K\eta_0 a_0 10^{-0.5a_0},$$

where a_0 is the absorbance at the excitation wavelength (365 nm), and K is the apparatus function. After measurement of the absorbance and PL intensity of the sample using the same apparatus parameters, the PL efficiency of the sample was derived by comparing its PL intensity with that of the standard quinine solution. The error in the PL efficiency was estimated to be within 10 % by comparing the results using two standards: quinine and R6G.

Results and discussion

The growth process of CdSe cores was controlled by reaction conditions. To create CdSe cores with various sizes, reaction time and the injection speed of TOPSe were optimized. Figure 1 shows the TEM images of CdSe cores using different injection speed of TOPSe and reaction time. The average diameter of CdSe cores increased with time under a low injection speed. This is ascribed to the time dependence of nucleation and growth of CdSe. In the

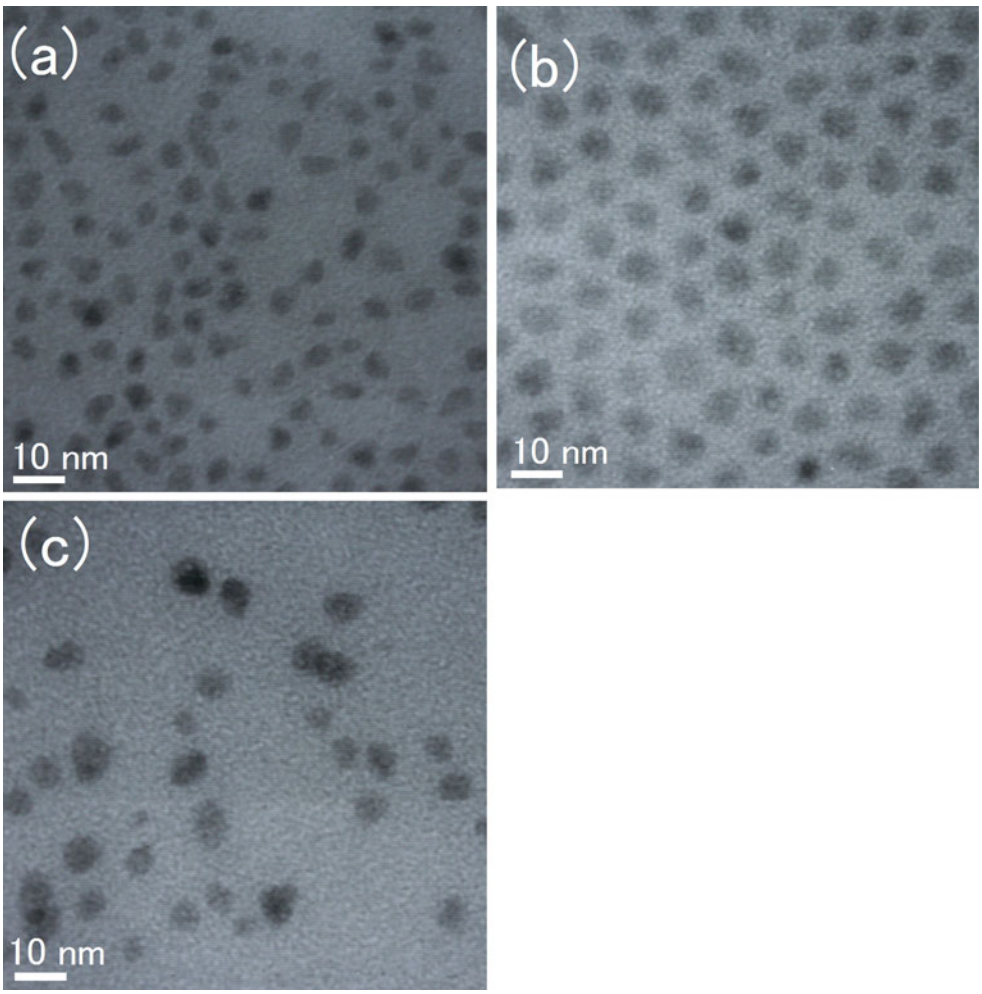

Fig. 5 TEM images of CdSe cores and them with a CdZnS and ZnS shell shown in Table 2. **a** Sample 3 (CdSe cores). **b** Sample 8 (CdSe/$Cd_{1-x}Zn_xS$). **c** Sample 9 (CdSe/ZnS)

case of quick TOPSe injection and short reaction time (Sample 1), large amount of CdSe nuclei quickly formed and grew into small cores. In contrast, small amount of CdSe nuclei formed and subsequently grew into large cores when the slow TOPSe injection speed (Sample 2) was used. Sample 3 revealed a rod-like morphology as shown in Fig. 5a. Table 1 summarized the preparation conditions and properties of CdSe cores.

CdSe cores revealed strong size dependence of optical properties which have been monitored to reflect mean particle size and size distribution through the temporal evolution of UV–Vis and PL spectra. Figure 2 displays the absorption and PL spectra of CdSe cores (Samples 1 and 2 shown in Table 1). Compared with Sample 1, Sample 2 revealed red-shifted absorption and PL peak. However, the PL of Sample 2 was weak. The preparation of the cores revealed a good re-reducibility. The homogeneous injection of TOPSe was a key for cores with narrow size distribution, in which new nucleation can be prevented during particle growth.

According to our previous experiments [17], an optimal molar ratio of Cd/Zn of 1/1 was used for CdSe cores coated with a $Cd_xZn_{1-x}S$ shell to obtain high PL efficiencies. Figure 3 shows the TEM image of CdSe cores with a $Cd_{1-x}Zn_xS$ and ZnS shell shown in Table 2: (a) Sample 4 (CdSe/$Cd_{1-x}Zn_xS$), (b) Sample 5 (CdSe/ZnS), (c) Sample 6 (CdSe/$Cd_{1-x}Zn_xS$), and (d) Sample 7(CdSe/ZnS). Table 2 illustrates the preparation condition and properties of core/shell CdSe/$Cd_xZn_{1-x}S$ and CdSe/ZnS QDs fabricated by using Samples 1–3 shown in Table 1. Although two samples were prepared by the same shell coating process, Sample 6 exhibited a cubic morphology, while Sample 4 revealed a spherical shape. This is ascribed to the difference of CdSe cores. In contrast, spherical QDs were observed both in the TEM images of Samples 5 and 7 even though they were created by using different CdSe cores (Samples 1 and 2). This is ascribed to the growth kinetics of ZnS and $Cd_xZn_{1-x}S$ shells.

The crystal structures of CdSe exhibit two polymorphic forms, namely, cubic and hexagonal phases, depending on the synthesis conditions and methods. Usually to obtain the

pure hexagonal phase CdSe, sufficiently higher reaction temperature and longer reaction time are needed [17]. Due to the lattice mismatch between the core and the shell, the interface strain accumulates dramatically during the shell-growth, and eventually can be released through the formation of dislocations, indicating that the spatial distribution of defects in core–shell QDs can be controlled by the shell-growth. The large mismatch (ca. 12 %) between CdSe and ZnS lattice parameters induces the strain at the interface between the core and the shell [20]. In the case of CdSe/CdS, the lattice mismatch between the core and the shell materials is relatively small. Therefore, a CdS interlayer was created when CdSe cores were coated with a $Cd_xZn_{1-x}S$ shell. Sample 6 (CdSe/$Cd_xZn_{1-x}S$ QDs) exhibited a cubic morphology. This means the anisotropic deposition of CdS on the cores occurs during the shell-growth. A CdS shell grew preferentially on the $\{00\bar{1}\}$ facet of CdSe cores. $Cd_xZn_{1-x}S$ shells did not prefer to grow on the reactive {002} planes at the CdSe cores. Similar growth kinetics was used to prepare colloidal CdS, CdSe, and CdTe quantum rods and quantum rod heterostructures [21, 22]. Because of the surface states of a small CdSe core, the anisotropic deposition of CdS did not occur. Therefore, spherical QDs were observed in the TEM image of Sample 4. In the case of a ZnS shell, the anisotropic deposition of ZnS became difficult because of a large lattice mismatch.

Because the spatial distribution of defects in core/shell QDs can be controlled by the shell-growth, the series of PL spectra from QDs with successive shell-growth can reveal the nature of traps in QDs. To indicate the dependence of PL properties on composition and morphology, Fig. 4 shows absorption and PL spectra of CdSe cores coated with a $Cd_{1-x}Zn_xS$ and ZnS shell: (a) Samples 4 (CdSe/$Cd_{1-x}Zn_xS$) and 5 (CdSe/ZnS), (b) Samples 6 (CdSe/$Cd_{1-x}Zn_xS$) and 7 (CdSe/ZnS). A significant red-shift was observed in both the absorption and PL spectra of the core–shell QDs in contrast to those of CdSe cores. This was an indication of the formation of a core–shell structure. However, the red-shifted degree became small in the case of a ZnS shell instead of a $Cd_xZn_{1-x}S$ shell. After coating with a shell, the PL efficiency of the QDs was greatly enhanced. This is ascribed that the shell-growth can eliminate nonradiative defects on the core's surface. The full-width at half-maximum (FWHM) of PL spectra of the core/shell QDs was similar to that of CdSe core. All the core/shell QDs exhibited narrow PL spectra. This is utilizable for further applications such as biolabels.

To get core/shell QDs with long PL peak wavelength, large cores were created by a seeded growth technique. Figure 5 shows the TEM images of CdSe cores and CdSe cores with a CdZnS and ZnS shell shown in Tables 1 and 2: (a) Sample 3 (CdSe cores), (b) Sample 8 (CdSe/$Cd_{1-x}Zn_xS$), and Sample 9 (CdSe/ZnS). Sample 3 (CdSe cores) exhibited a rod-like morphology. Because the PL efficiency of Sample 3 is higher than that of Sample 2 (CdSe cores), the cores was benefit for the seeded growth technique. CdSe nanorod growth can be promoted by inducing a burst of particle nucleation and then adding more reactant at low supersaturation to alleviate further particle nucleation and favor epitaxial deposition on the {002} surfaces, which appears to be the most reactive facet of the nanorods [13]. In our experiments, the growth of rod-like CdSe was carried out using small CdSe cores as seeds by controlling the injection speed of TOPSe. The anisotropic aggregation behaviors of CdSe monomers on the small CdSe seeds occur by adding reactant at low supersaturation. The slow injection of TOPSe prevented CdSe QDs from new nucleation.

Samples 8 (CdSe/$Cd_{1-x}Zn_xS$) shown in Fig. 5 exhibited a spherical morphology with an average size of 7.5 nm in diameter. This differs in that of Sample 6 (cubic morphology) shown in Fig. 3. The size increase in length of the

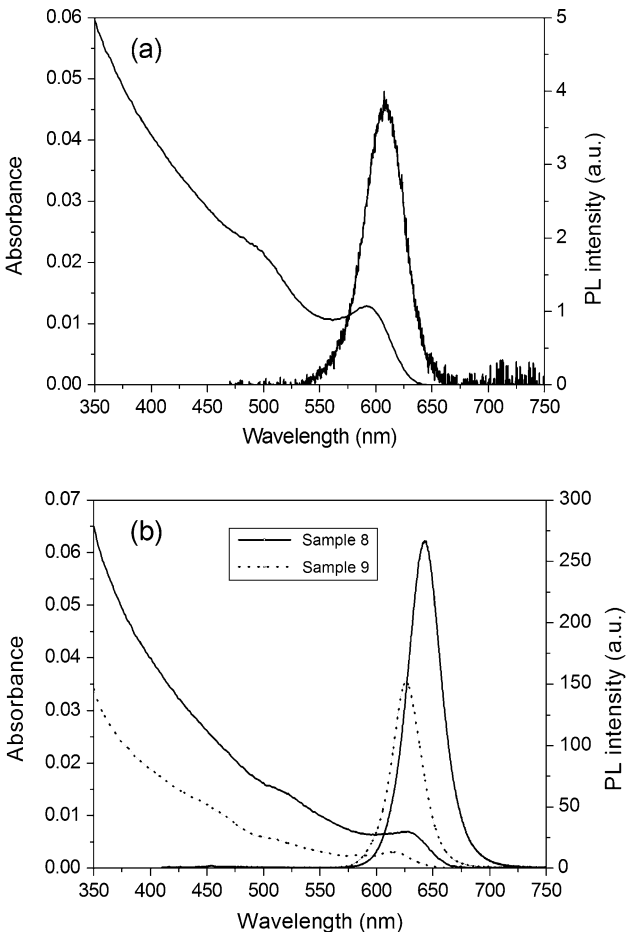

Fig. 6 Absorption and PL spectra of CdSe cores and them with a $Cd_{1-x}Zn_xS$ and ZnS shell shown in Table 2. **a** Sample 3 (CdSe cores). **b** Sample 8 (CdSe/$Cd_{1-x}Zn_xS$) and Sample 9 (CdSe/ZnS)

QDs is smaller than that in their diameter. This is ascribed CdS interlayers grow preferentially on the $\{00\bar{1}\}$ facet of CdSe rod-like cores. In other words, Cd, Zn, and S monomers are being added to both the unique *c*-axis facet and the facets representative of the diameter of the rod-like CdSe cores simultaneously. In contrast, the size distribution of Sample 9 (CdSe/ZnS) became broad even though the figure is revealed a spherical shape. The result indicates the growth behavior of a ZnS shell is different from that of a $Cd_{1-x}Zn_xS$ shell.

Figure 6 shows the absorption and PL spectra of CdSe cores and the cores coated with a CdZnS and ZnS shell shown in Table 2: (a) Sample 3 (CdSe cores), (b) Sample 8 (CdSe/$Cd_{1-x}Zn_xS$), and Sample 9 (CdSe/ZnS). Sample 3 revealed a PL peak wavelength of 607 nm and a FWHM of PL spectrum of 40.8 nm. Compared with Sample 1 (seeds, 3.3 nm in diameter), Sample 3 revealed a red-shift both in absorption and PL spectra. Red-shifting of the excitonic peak is confined the diameter (4.1 nm) of rod-like CdSe QDs, and is not defined by the length (5.9 nm) of rod-like CdSe QDs. This red-shifting is also indicative of the dynamic increase of the QD diameter during the growth period. After a shell coating, QDs revealed increased PL efficiency and red-shifted absorption and PL spectra. However, the red-shifted degree of PL spectra of Samples 8 and 9 were 36 and 20 nm, respectively. This is ascribed to the effect of composition on the band gap of QDs.

Conclusions

We have described two ways including direct organic synthesis and a seeded growth procedure by adding reactant slowly to fabricated CdSe cores with various sizes and morphologies. The cores revealed spherical and rod-like morphologies. $Cd_{1-x}Zn_xS$ and ZnS shells were subsequently coated through an organic synthesis at relatively low temperature using HDA as a capping agent. In the case of small CdSe cores (3.3 nm in diameter), the core/shell QDs revealed a spherical morphology, in which anisotropic growth of shells did not occur. However, the core/shell QDs exhibited a cubic morphology with a length of 5 nm once middle size CdSe cores (3.9 nm in diameter) are used instead of small one. As for CdSe cores with a rod-like morphology, the anisotropic growth of $Cd_{1-x}Zn_xS$ shells resulted in the creation of spherical core/shell QDs with an average size of 7.5 nm in diameter. The size increase in length of the QDs is smaller than that in their diameter. After coating with a ZnS shell, all core/shell CdSe/ZnS QDs prepared using different kinds of cores exhibited a spherical morphology. This indicates the anisotropic deposition depended strongly on a CdS inter layer. Although core/shell QDs with $Cd_{1-x}Zn_xS$ and ZnS shells revealed a red-shift both in absorption and PL spectra, the red-shifted degree of CdSe/$Cd_{1-x}Zn_xS$ QDs became large. This is ascribed to the composition effect on the band gap of semiconductor. In the case of rod-like CdSe cores, core/shell CdSe/$Cd_{1-x}Zn_xS$ QDs revealed a red PL with a PL peak wavelength of 643 nm. Because of tunable PL and facile synthesis at relatively low temperature, the reported approach is suitable for production of high-quality CdSe based core/shell QDs, especially for large, red-emitting ones, due to its easy scale-up, high reproducibility, and low cost.

References

1. Huynh WU, Dittmer JJ, Alivisatos AP (2002) Science 295:2425
2. Sitt A, Salant A, Menagen G, Banin U (2011) Nano Lett 11:2054
3. Hu JT, Li LS, Yang WD, Manna L, Wang LW, Alivisatos AP (2001) Science 292:2060
4. Wolcott A, Fitzmorris RC, Muzaffery O, Zhang JZ (2010) Chem Mater 22:2814
5. Sitt A, Della Sala F, Menagen G, Banin U (2009) Nano Lett 9:3470
6. Dorfs D, Salant A, Popov I, Banin U (2008) Small 4:1319
7. Li JJ, Wang YA, Guo WZ, Keay JC, Mishima TD, Johnson MD, Peng XG (2003) J Am Chem Soc 125:12567
8. Steckel JS, Zimmer JP, Coe-Sullivan S, Stott NE, Bulovic V, Bawendi MG (2004) Angew Chem Int Ed 43:2154
9. Huang GW, Chen CY, Wu KC, Ahmed MO, Chou PT (2004) J Cryst Growth 265:250
10. Chou PT, Chiu YH (2004) J Phys Chem B 108:10687
11. Talapin DV, Mekis I, Gotzinger S, Kornowski A, Benson O, Weller H (2004) J Phys Chem B 108:18826
12. Sheng Q, Kim S, Lee J, Kim SW, Jensen K, Bawendi MG (2006) Langmuir 22:3782
13. Manna L, Scher EC, Alivisatos AP (2000) J Am Chem Soc 122:12700
14. Manna L, Milliron DJ, Meisel A, Scher EC, Alivisatos AP (2003) Nat Mater 2:382
15. Fu AH, Gu WW, Boussert B, Koski K, Gerion D, Manna L, Le Gros M, Larabell CA, Alivisatos AP (2007) Nano Lett 7:179
16. Yong KT, Qian J, Roy I, Lee HH, Bergey EJ, Tramposch KM, He SL, Swihart MT, Maitra A, Prasad PN (2007) Nano Lett 7:761
17. Yang P, Ando M, Taguchi T, Murase N (2011) J Phys Chem C 115:14455
18. Murase N, Li C (2008) J Lumin 128:1896
19. Zeng Q, Kong X, Sun Y, Zhang Y, Tu L, Zhao J, Zhang H (2008) J Phys Chem C 112:8587
20. Talapin DV, Mekis I, Götzinger S, Kornowski A, Benson Q, Weller H (2004) J Phys Chem B 108:18829
21. Shieh F, Saunders AE, Korgel BA (2005) J Phys Chem B 109:8538
22. Deka S, Quarta A, Lupo MG, Falqui A, Boninelli S, Giannini C, Morello G, De Giorgi M, Lanzani G, Spinella C, Cingolani R, Pellegrino T, Manna L (2009) J Am Chem Soc 131:2948